NASA TM X- 70623

SOLAR ENERGY MONITOR IN SPACE (SEMIS)

MATTHEW P. THEKAEKARA

MARCH 1974

GSFC —— **GODDARD SPACE FLIGHT CENTER** ——
GREENBELT, MARYLAND

SOLAR ENERGY MONITOR IN SPACE (SEMIS)

by

Matthew P. Thekaekara
Upper Atmosphere Branch
Atmospheric and Hydrospheric Applications Division

March 1974

GODDARD SPACE FLIGHT CENTER
Greenbelt, Maryland

SOLAR ENERGY MONITOR IN SPACE (SEMIS)*

M. P. Thekaekara

NASA/Goddard Space Flight Center

Greenbelt, Maryland 20771

ABSTRACT

Measurements made at high altitudes from aircraft have resulted in the establishment of standard values of the solar constant and extraterrestrial solar spectral irradiance. They have been adopted as the engineering standard by the American Association of Testing and Materials (ASTM) and as design values for the NASA Space Vehicles Design Criteria. These standard values and other solar spectral curves which were derived from these for practical applications are described. The problem of possible variations of the solar constant and solar spectrum and their influence on the Earth-atmosphere system and weather related phenomena is examined. It is shown that the solar energy input parameters should be determined with considerably greater accuracy and precision than has been hitherto possible. A measurement program which is currently being planned for this purpose and the instrumentation which is being developed will be described. The instrument package is designed as a compact, low weight solar energy monitor in space (SEMIS). Preliminary measurements will be made at 20 km altitude from the U-2 aircraft. More advanced versions of the SEMIS will be flight-tested on balloons and aircraft for installation eventually in the Space Shuttle.

CONTENTS

ILLUSTRATIONS

ILLUSTRATIONS (continued)

TABLES

1. THE SOLAR CONSTANT AND THE SOLAR SPECTRUM

We shall present first the data on the solar constant and solar spectrum which have been developed in recent years in the United States. This will show the inadequacy of available data and the need for a program such as the SEMIS.

Since the advent of satellites and high altitudes research aircraft several attempts were made to measure the solar constant from above all or almost all of the Earth's atmosphere. An ad hoc committee on Solar Electromagnetic Radiation was appointed by the NASA Space Vehicles Design Criteria Office and by the Institute of Environmental Sciences to study this question. The Committee made a detailed survey of all available information and recommended standard values for the solar constant and the extraterrestrial solar spectrum. The solar constant was evaluated from nine series of measurements, all made from high altitude platforms, namely, Convair 990 and B-57B jet aircraft, X-15 rocket aircraft, balloons and Mariner Mars probe.

These nine values are shown in Table I. Each one of these is the result of many series of measurements. The uncertainties claimed by the authors are shown in the last column. The values are referenced to three different radiation scales: the International Pyrheliometric Scale of 1956 (IPS 56), the Absolute Electrical Units Scale (AEUS) and the Thermodynamic Kelvin Temperature Scale (TKTS). The differences in values may be due to basic differences in radiation scales, calibration errors of each instrument, errors in extrapolation to air mass zero, window transmittance, scattered light and other causes. The

1

Table I

High Altitude Determinations of the Solar Constant

Platform	Detector	Reference Scale of Radiometry	Solar Constant W m^{-2}	Estimated Error ±W m^{-2}
Balloon[1] U. of Denver Expt.	Normal incidence pyrheliometer	IPS 56	1338	6
CV 990[2] GSFC Expt.	Ångström 6618	IPS 56	1343	26
CV 990[2] GSFC Expt.	Ångström 7635	IPS 56	1349	40
CV 990[2] GSFC Expt.	Hycal pyrheliometer	TKTS	1352	22
Mariner 6 and 7 Spacecraft, JPL[3]	Cavity radiometer	AEUS	1353	10
Balloon, U. of Leningrad Expt.[4]	U. of Leningrad actinometer	IPS 56	1353	14
CV 990[2] GSFC Expt.	Cone radiometer	AEUS	1358	24
CV 990, B-57B, X-15 Eppley-JPL Expt.[5,6,7]	Eppley pyrheliometer	IPS 56	1360	13
Balloon, JPL Expt.[8]	Active Cavity radiometer	AEUS	1368	7
Standard Value			1353	21

Goddard experimenters had also another value obtained by integrating the value under the spectral curve, 1352 W m^{-2}. That this was so close to the average was assumed to be fortuitous rather than warranted by the accuracy of the spectral data. So this value was not included in the list selected for averaging. The detectors included Ångström pyrheliometers, cavity radiometers, and normal incidence pyrheliometers of different types and manufacturers. The value of the solar constant derived from these measurements was 1353 W m^{-2} or 1.940 cal cm^{-2} min^{-1}.

The solar spectral irradiance was obtained mainly from measurements made by NASA GSFC experimenters at an altitude of 11.6 km from a Convair 990 jet aircraft.[2] In Table II are listed the spectroradiometric instruments used on the CV 990. Along with each instrument is shown the disperser, the aircraft window material, the energy detector, and the wavelength range. The main standard of calibration was a set of five 1000 W quartz iodine lamps calibrated at the National Bureau of Standards or the Eppley Laboratory. These were supplemented in the long wavelength range by two blackbody sources operating at 1200 K and 3000 K. As shown in Table II, there were two large prism mono-chromators, a filter radiometer (33 filters, each 100 A bandwidth) and two inter-ferometers. The spectral irradiance curve obtained from these detailed meas-urements was modified slightly in the visible range with the aid of data from the multi-channel filter radiometers flown by the Eppley-JPL Team under the direc-tion of A. J. Drummond.[5,6,7] The GSFC results cover the spectral range

Table II

Spectral Irradiance Instruments on board CV 990 NASA 711 Aircraft

Instrument	Spectral Dispersion by	Aircraft Window Material	Energy Detector	Wavelength Range
Perkin-Elmer monochromator	Lithium fluoride prism	Sapphire	1 P 28 Phototube Thermocouple	0.3 – 0.7 μm 0.7 – 4.0 μm
Leiss double prism monochromator	Two quartz prisms	Dynasil quartz	EMI 9558 QA Tube PbS tube	0.3 – 0.7 μm 0.7 – 1.6 μm
Filter radiometer	33 Dielectric thin film filters	Dynasil quartz	RLA type 917 phototube (S-1)	0.3 – 1.2 μm
P-4 polarization type interferometer	Soleil prism	Infrasil quartz	1 P 28 or R 136 Tube PbS tube	0.3 – 0.7 μm 0.7 – 2.5 μm
I-4 moving mirror type interferometer	Michelson mirror	Intran 4	Thermistor bolometer	2.6 – 15.0 μm

4

0.3 to 15 μm which contains nearly 99 percent of the Sun's energy. Data from other sources were added for the two extreme ends of the spectrum, from Heath[9] and Hinteregger[10] for the UV and from Shimabukoro and Stacey[11] for the IR beyond 15 μm.

The spectral curve which was derived from the GSFC data and the Eppley-JPL data is shown in Figure 1. The wavelength range is 0.2 to 2.6 μm. The solar spectral irradiance values for the wavelength range 0.115 to 1000 μm is given in Table III. The columns are wavelength, spectral irradiance E_λ, area under the curve 0 to λ and % area. The values of E_λ are averages over 100 A for most of the range.
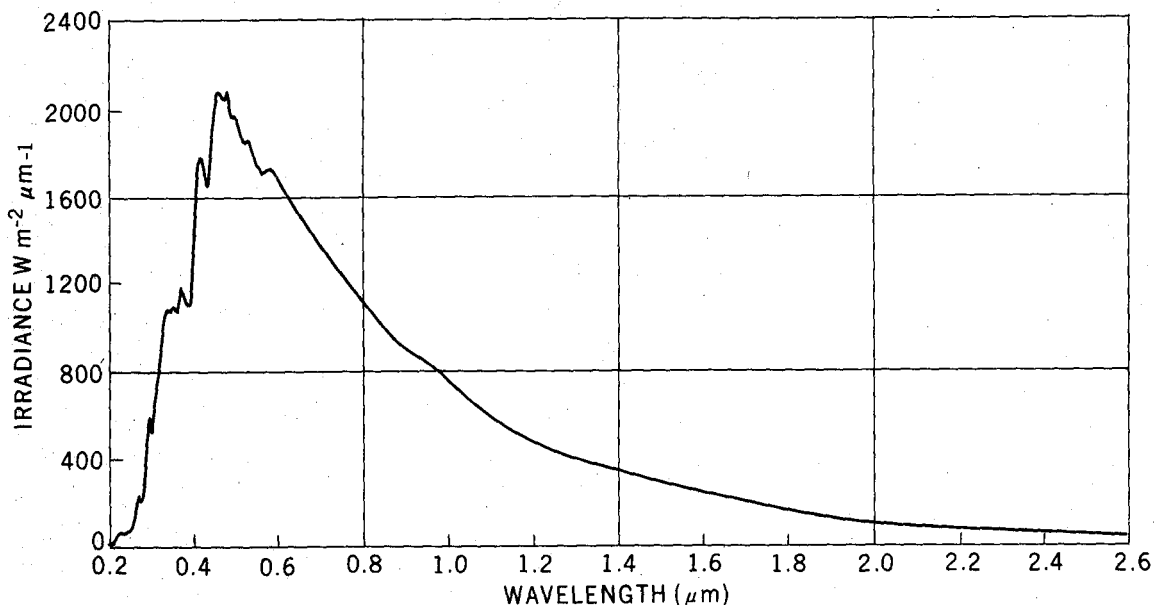
Figure 1. The NASA/ASTM standard curve of extraterrestrial solar spectral irradiance, 0.2 to 2.6 μm.

Table III. Solar Spectral Irradiance – Standard Curve

λ – Wavelength in micrometers

E_λ – Solar spectral irradiance averaged over small bandwidth centered at λ, in $W\ m^{-2}\ \mu m^{-1}$

$E_{o-\lambda}$ – Integrated solar irradiance in the wavelength range o to λ, in $W\ m^{-2}$

$D_{o-\lambda}$ – Percentage of solar constant associated with wavelengths shorter than λ

Solar constant – 1353 $W\ m^{-2}$

Note: lines indicate change in wavelength interval of integration

λ	E_λ	$E_{o-\lambda}$	$D_{o-\lambda}$	λ	E_λ	$E_{o-\lambda}$	$D_{o-\lambda}$	λ	E_λ	$E_{o-\lambda}$	$D_{o-\lambda}$
.115	.007	.0025	.0001	.510	1882	324.926	24.015	1.55	267	1186.109	87.665
.120	.900	.0048	.0003	.515	1833	334.214	24.701	1.60	245	1198.909	88.611
.125	.007	.0070	.0005	.520	1833	343.379	25.379	1.65	223	1210.609	89.475
.130	.007	.0071	.0005	.525	1852	352.591	26.059	1.70	202	1221.234	90.261
.140	.030	.0073	.0005	.530	1842	361.826	26.742	1.75	180	1230.784	90.967
.150	.070	.0078	.0005	.535	1818	370.976	27.418	1.80	159	1239.259	91.593
.160	.230	.0093	.0006	.540	1783	379.979	28.084	1.85	142	1246.784	92.149
.170	.630	.0136	.0010	.545	1754	388.821	28.737	1.90	126	1253.484	92.644
.180	1.250	.0230	.0016	.550	1725	397.519	29.380	1.95	114	1259.484	93.088
.190	2.710	.0428	.0031	.555	1720	406.131	30.017	2.00	103	1264.909	93.489
.200	10.7	.1098	.0081	.560	1695	414.669	30.648	2.1	90	1274.559	94.2024
.210	22.9	.2778	.0205	.565	1705	423.169	31.276	2.2	79	1283.009	94.8269
.220	57.5	.6798	.0502	.570	1712	431.711	31.907	2.3	69	1290.409	95.3739
.225	64.9	.9858	.0728	.575	1719	440.289	32.541	2.4	62	1296.959	95.8580
.230	66.7	1.3148	.0971	.580	1715	448.874	33.176	2.5	55	1302.809	96.2903
.235	59.3	1.6298	.1204	.585	1712	457.441	33.809	2.6	48	1307.959	96.6710
.240	63.0	1.9356	.1430	.590	1700	465.971	34.439	2.7	43	1312.509	97.0073
.245	72.3	2.2738	.1680	.595	1682	474.426	35.064	2.8	39	1316.609	97.3103
.250	70.4	2.6306	.1944	.600	1666	482.796	35.683	2.9	35	1320.309	97.5838
.255	104.0	3.0666	.2266	.605	1647	491.079	36.295	3.0	31	1323.609	97.8277
.260	130	3.6516	.269	.61	1635	499.284	36.902	3.1	26.0	1326.459	98.0383
.265	185	4.4391	.328	.62	1602	515.469	38.098	3.2	22.6	1328.889	98.2179
.270	232	5.4816	.405	.63	1570	531.329	39.270	3.3	19.2	1330.979	98.3724
.275	204	6.5716	.485	.64	1544	546.899	40.421	3.4	16.6	1332.769	98.5047
.280	222	7.6366	.564	.65	1511	562.174	41.550	3.5	14.6	1334.329	98.6200
.285	315	8.9791	.663	.66	1486	577.159	42.657	3.6	13.5	1335.734	98.7238
.290	482	10.9716	.810	.67	1456	591.869	43.744	3.7	12.3	1337.024	98.8192
.295	584	13.6366	1.007	.68	1427	606.284	44.810	3.8	11.1	1338.194	98.9056
.300	514	16.3816	1.210	.69	1402	620.429	45.855	3.9	10.3	1339.264	98.9847
.305	603	19.1741	1.417	.70	1369	634.284	46.879	4.0	9.5	1340.254	99.0579
.310	689	22.4041	1.655	.71	1344	647.849	47.882	4.1	8.70	1341.1641	99.12521
.315	764	26.0366	1.924	.72	1314	661.139	48.864	4.2	7.80	1341.9891	99.18618
.320	830	30.0216	2.218	.73	1290	674.159	49.826	4.3	7.10	1342.7341	99.24124
.325	975	34.5341	2.552	.74	1260	686.909	50.769	4.4	6.50	1343.4141	99.29150
.330	1059	39.6191	2.928	.75	1235	699.384	51.691	4.5	5.92	1344.0351	99.33740
.335	1081	44.9691	3.323	.76	1211	711.614	52.595	4.6	5.35	1344.5986	99.37905
.340	1074	50.3566	3.721	.77	1185	723.594	53.480	4.7	4.86	1345.1091	99.41678
.345	1069	55.7141	4.117	.78	1159	735.314	54.346	4.8	4.47	1345.5757	99.45127
.350	1093	61.1191	4.517	.79	1134	746.779	55.194	4.9	4.11	1346.0049	99.48299
.355	1083	66.5591	4.919	.80	1109	757.994	56.023	5.0	3.79	1346.3999	99.51219
.360	1068	71.9366	5.316	.81	1085	768.966	56.834	6	1.8200	1349.2049	99.71950
.365	1132	77.4366	5.723	.82	1060	779.694	57.627	7	.9900	1350.6099	99.82335
.370	1181	83.2191	6.150	.83	1036	790.174	58.401	8	.5850	1351.3974	99.88155
.375	1157	89.0641	6.582	.84	1013	800.419	59.158	9	.3670	1351.8734	99.91673
.380	1120	94.7566	7.003	.85	990	810.434	59.899	10	.2410	1352.1774	99.93920
.385	1098	100.3016	7.413	.86	968	820.224	60.622	11	.1650	1352.3804	99.95420
.390	1098	105.7916	7.819	.87	947	829.799	61.330	12	.1170	1352.5214	99.96462
.395	1189	111.5091	8.241	.88	926	839.164	62.022	13	.0851	1352.6224	99.97209
.400	1429	118.0541	8.725	.89	908	848.334	62.700	14	.0634	1352.6967	99.97758
.405	1644	125.7366	9.293	.90	891	857.329	63.365	15	.0481	1352.7524	99.98170
.410	1751	134.224	9.920	.91	880	866.184	64.019	16	.037100	1352.7950	99.98485
.415	1774	143.036	10.571	.92	869	874.929	64.665	17	.029100	1352.8281	99.98730
.420	1747	151.839	11.222	.93	858	883.564	65.304	18	.023100	1352.8542	99.98923
.425	1693	160.439	11.858	.94	847	892.089	65.934	19	.018600	1352.8751	99.99077
.430	1639	168.769	12.473	.95	837	900.509	66.556	20	.015200	1352.8920	99.99202
.435	1663	177.024	13.083	.96	820	908.794	67.168	25	.006170	1352.9454	99.99596
.440	1810	185.706	13.725	.97	803	916.909	67.768	30	.002970	1352.9683	99.99765
.445	1922	195.036	14.415	.98	785	924.849	68.355	35	.001600	1352.9797	99.99850
.450	2006	204.856	15.140	.99	767	932.609	68.928	40	.000942	1352.9860	99.99897
.455	2057	215.014	15.891	1.00	748	940.184	69.488	50	.000391	1352.9927	99.99946
.460	2066	225.321	16.653	1.05	668	975.584	72.105	60	.00019000	1352.9956	99.99967
.465	2048	235.606	17.413	1.10	593	1007.109	74.435	80	.00006160	1352.9981	99.99986
.470	2033	245.809	18.167	1.15	535	1035.309	76.519	100	.00002570	1352.9990	99.99992
.475	2044	256.001	18.921	1.20	485	1060.809	78.404	120	.00001260	1352.9994	99.99995
.480	2074	266.296	19.681	1.25	438	1083.884	80.109	150	.00000523	1352.9997	99.99997
.485	1976	276.421	20.430	1.30	397	1104.759	81.652	200	.00000169	1352.9998	99.99999
.490	1950	286.236	21.155	1.35	358	1123.634	83.047	250	.00000070	1352.9999	99.99999
.495	1960	296.011	21.878	1.40	337	1141.009	84.331	300	.00000034	1352.9999	99.99999
.500	1942	305.766	22.599	1.45	312	1157.234	85.530	400	.00000011	1352.9999	99.99999
.505	1920	315.421	23.312	1.50	288	1172.234	86.639	1000	.00000000	1353.0000	100.00000

6

The whole of the solar electromagnetic spectrum from 10 A to 10 m is shown in Figure 2. There are 10 decades on the wavelength scale. The irradiance scale changes 3 times in the IR each time by 10^6. The Sun is a variable star in the radio range near 1 m and in the UV. The dashed lines show Planckian curves at equivalent blackbody temperature, which is 5762 K over most of the range but goes to higher values at the two extremes.

Following the recommendation of the Committee on Solar Electromagnetic Radiation, these values have received a wide circulation and have been extensively used as a standard of reference. A monograph[12] published in the NASA Space Vehicles Design Criteria series recommends these values as criteria for design and testing of spacecraft systems. These values have been adopted by the Solar Simulation Committee of the Institute of Environmental Sciences and have been developed by the American Society for Testing and Materials (ASTM) into an "Engineering Standard for the Solar Constant and Solar Spectrum[13]." A practical application which incidentally gave the first impetus to the GSFC Convair 990 project is the design of solar simulators and pre-launch testing of satellites and spacecraft components. In the laboratories of NASA, ESRO and their contractors the new values have replaced the older Johnson[14] values. One of the major suppliers of solar simulators, Spectrolab, Inc. of Sylmar, California, has issued for the convenience of users a wallet size card presenting the data. The standard solar spectral irradiance table is available in the current edition of the American Institute of Physics Handbook[15] and in the forthcoming Van Nostrand-Reinhold Encyclopedia of Physics. The chapter on Solar Radiation in
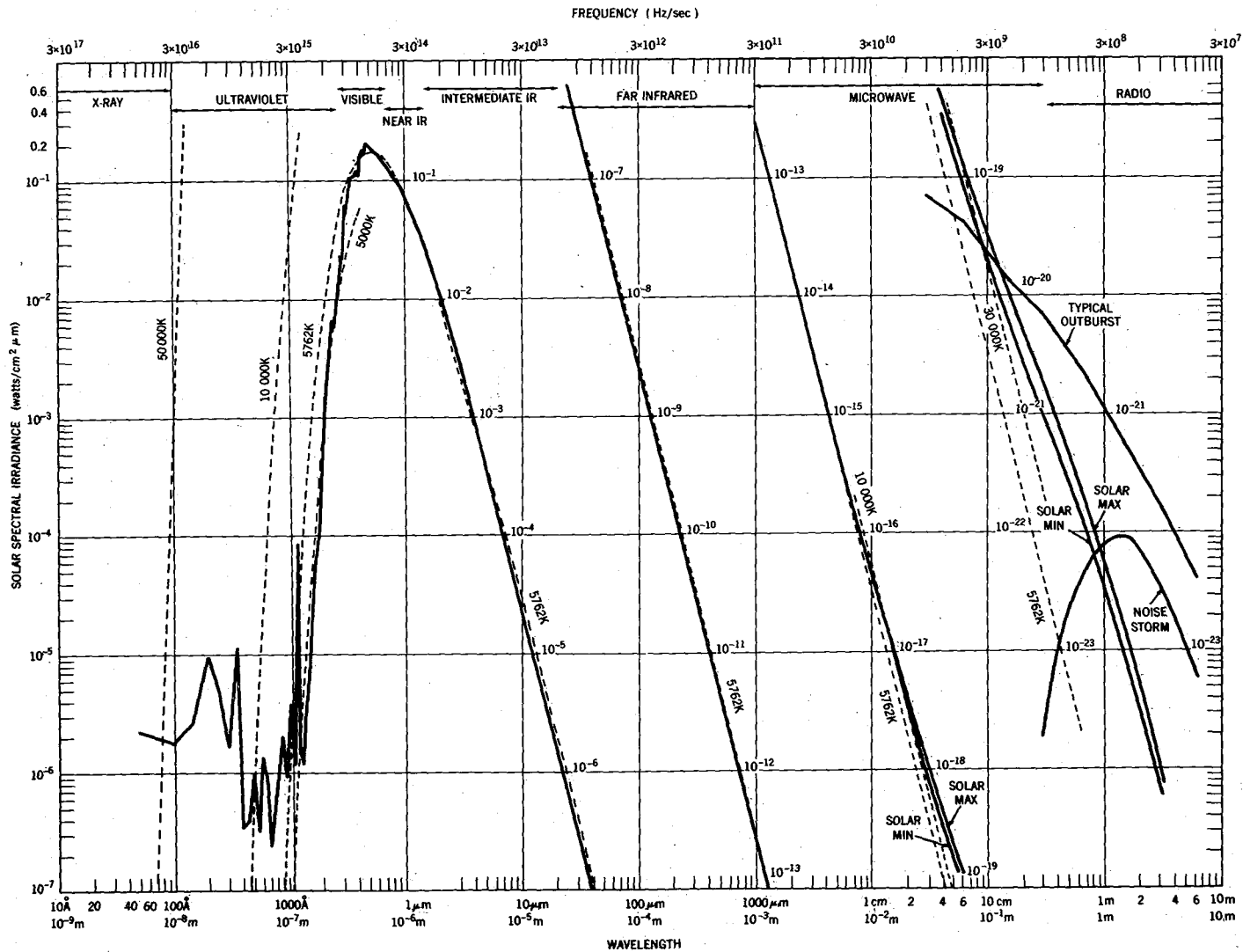
Figure 2. The extraterrestrial solar spectrum from X-rays to radio waves.

the AFCRL Handbook of Geophysics and Space Environments is in process of

revision to incorporate these data. Typical of the new curves to be published in

the AFCRL Handbook is Figure 3 which gives irradiance also at ground level of

air mass 1, 4, 7 and 10; i.e., for solar zenith angles 0, 75°, 82° and 84°. These

curves are for US standard atmosphere, ozone = 3.4 mm, precipitable water
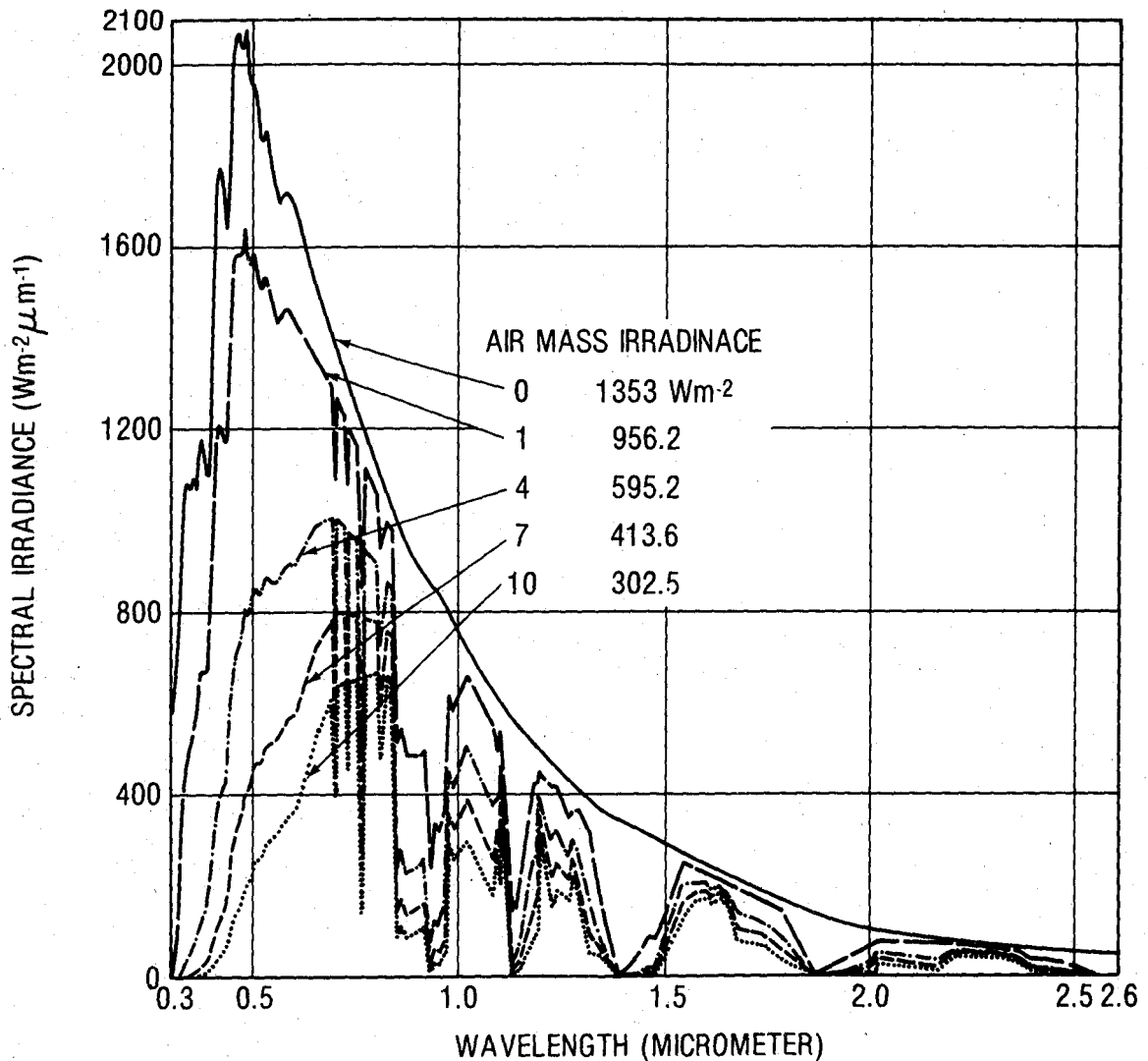
Figure 3. Solar irradiance spectra at ground level for air mass 1, 4, 7 and 10,
compared to the standard curve - computed values.

vapor = 20 mm, relatively clear air with turbidity coefficients, α = 1.3, β = 0.02. Elterman's values are assumed for extinction optical thickness due to Rayleigh scattering and ozone absorption[16]. For aerosol scattering (turbidity) the optical thickness is assumed to be of the form $\tau = \frac{\beta}{\lambda^\alpha}$. For absorption due to water vapor and other molecules the coefficients derived by Gates and Harrop[17] have been used. The program for computing these values for irradiance at ground level and for punching the cards was developed by D. Hoyt of NOAA, Boulder, Colorado.

Solar spectral irradiance values in Table III are listed at intervals of 50 A for the visible and near UV, and are averages over 100 A bandwidth centered at the given wavelength. This method of listing was chosen so as not to make the table too long and to give a spectrum independent of the Fraunhofer absorption which different instruments portray differently according to their resolution. For many applications like atmospheric modelling, pollution studies, transmittance computations of interference filters, studies of absorptive processes in the atmosphere, etc., a more detailed knowledge of the extraterrestrial solar spectrum was found to be necessary. In response to inquiries from users a project was undertaken recently to meet this need. For the wavelength range 3000 to 6100 A tables and charts are now available which give the spectrum at intervals of 1 A.

One of the curves for the range 3000 to 4000 A is shown in Figure 4. It is based on the data of the Perkin-Elmer monochromator on board the CV 990 aircraft. The spectral curve was read at 1 A intervals and cards were punched by

10
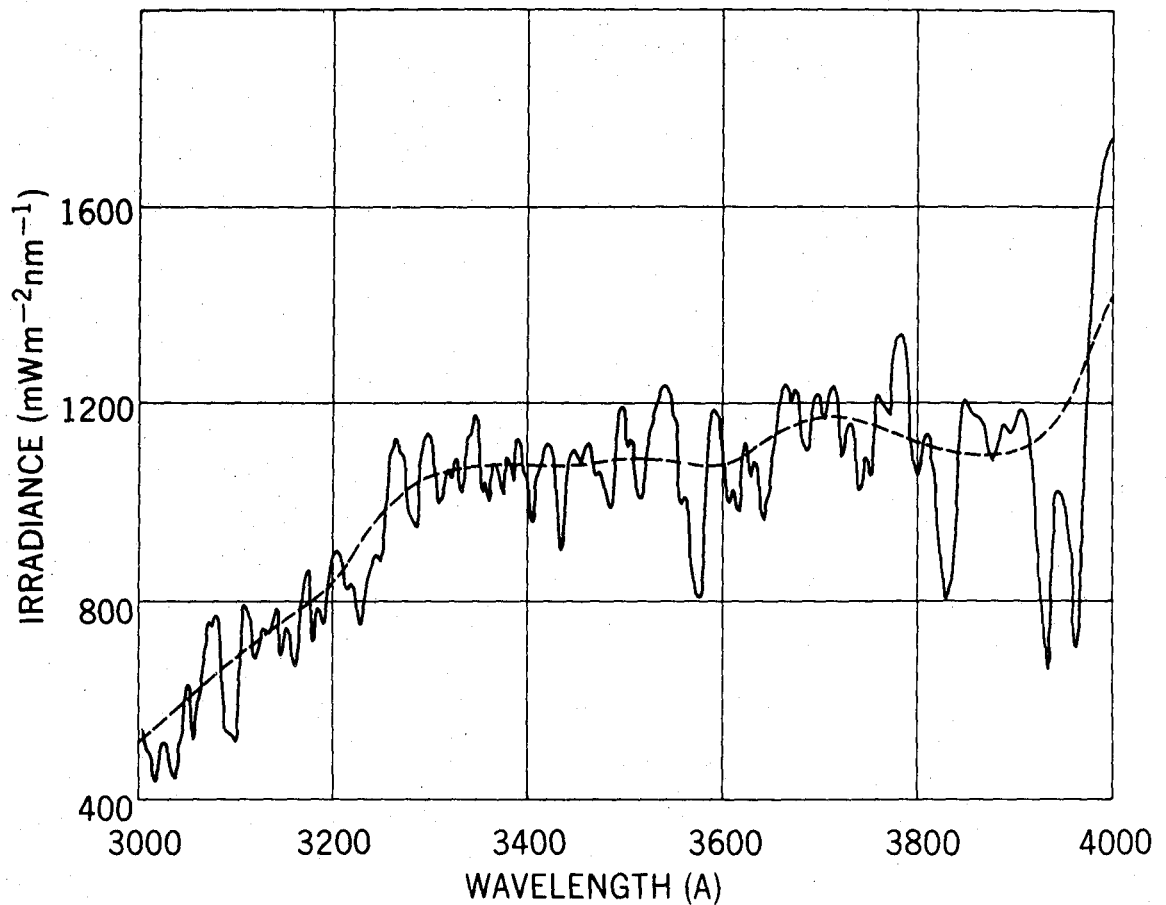
Figure 4. Solar spectrum obtained with a Perkin-Elmer monochromator, air
mass zero, 3000 - 4000 A.

J. DeLuisi of NCAR. We developed a normalization program so that in each

50 A range the integral under this curve is equal to the values of the standard

spectrum (Table III). The dashed line shows the standard curve. The curve

for the range 3600 to 6100 is shown in Figure 5. The well known solar absorp-

tion Ca^+ H and K lines at 3969 A and 3934 A respectively, the H_α line at 4861 A,

the Fe G line at 4308, etc., are readily recognizable on this curve.

11
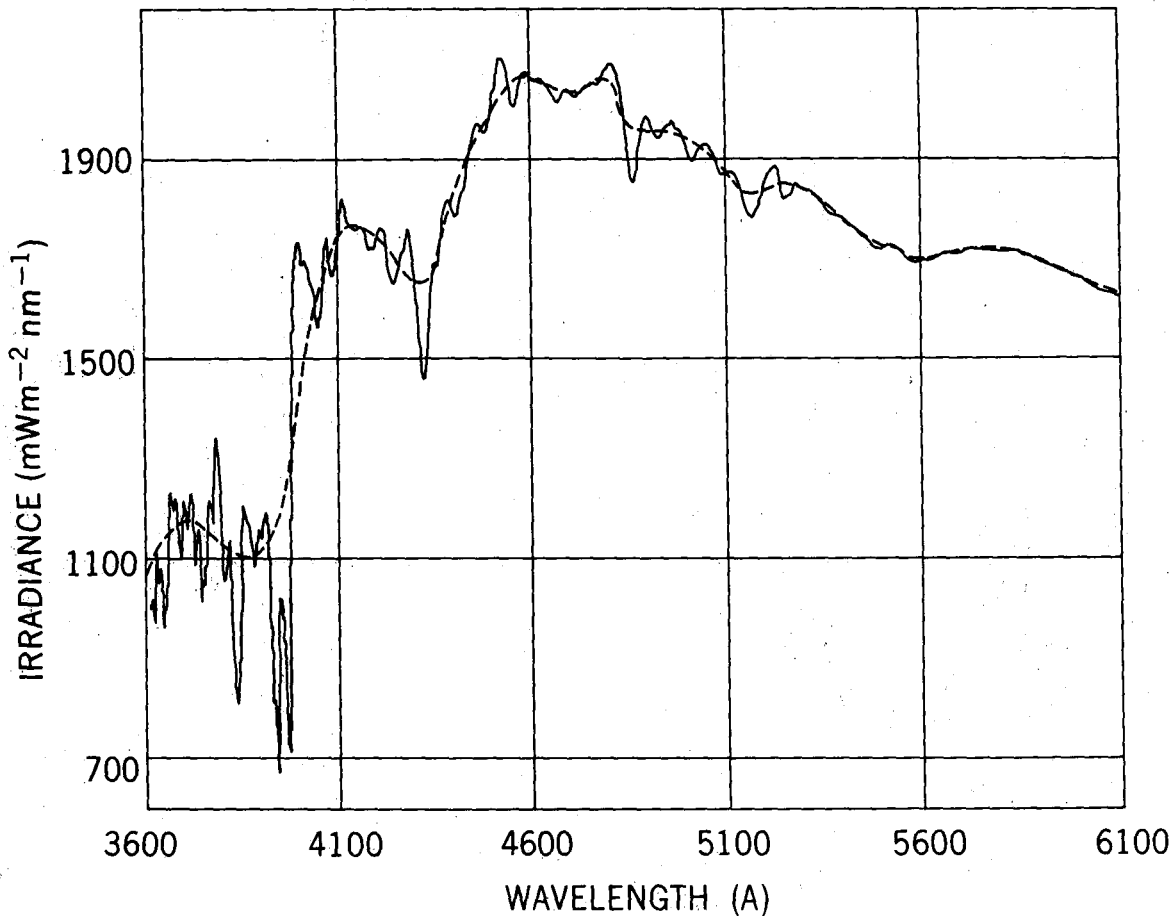
Figure 5. Solar spectrum obtained with a Perkin-Elmer monochromator, air mass zero, 3600 - 6100 A.

Punched cards giving solar spectral irradiance data (λ and E_λ) are available for the tables and figures discussed earlier, the standard table (Table III), spectral curves at ground level for several sets of atmospheric parameters and the extraterrestrial solar spectrum, 3000 to 6100 A, at one A intervals. User organizations which have need of such data for computer aided applications may obtain them by writing to the National Space Science Data Center, Code 601, NASA/GSFC, Greenbelt, Maryland 20771.

2. UNCERTAINTIES IN CURRENTLY AVAILABLE DATA

In many applications of solar irradiance data, solar and spectral, there are two questions of major importance, the absolute accuracy and the variability of these values.

As for the absolute accuracy of the solar constant there are several major problems. The values given in Table I based on high altitude measurements vary between a maximum of $1338\,W\,m^{-2}$ and $1368\,W\,m^{-2}$. The two extreme values are those which claim the least estimated error. The standard value adopted by NASA and ASTM is $1353\,W\,m^{-2}$ with an estimated uncertainty of $\pm21\,W\,m^{-2}$. For applications in meteorology, atmospheric physics, solar physics, etc., an absolute accuracy of the order of 0.1% or $\pm1.4\,W\,m^{-2}$ is desirable and many authors believe that it is possible within the state-of-the-art of radiometric measurements. Variations in the solar constant with sporadic or cyclic variations of the Sun itself cannot be detected unless the precision, if not the absolute accuracy, of the solar constant is 0.1% or better.

The values of the solar constant derived from ground-based measurements are significantly higher than $1353\,W\,m^{-2}$. F. S. Johnson's[14] value which was published in 1954 and had long been accepted as a standard in the U.S. was $1395\,W\,m^{-2}$ or 3.1% higher. Nicolet's value[18] was close to this, $1380\,W\,m^{-2}$. Still higher are the values derived by Stair and Johnston[19], $1428\,W\,m^{-2}$, and by Makarova and Kharitonov[20], $1418\,W\,m^{-2}$. In a recent monograph, "Distribution of Energy in the Solar Spectrum and the Solar Constant" published in Moscow[21],

Makarova and Kharitonov have proposed a value 1360 W m^{-2}; this is a weighted average of all the earlier measurements by many different authors. In 1968 Labs and Neckel[22] derived the value 1366 W m^{-2} based on measurements they made from Jungfraujoch in the wavelength range 0.33 to 1.25 μm and data from other authors for the region outside their range. In 1970[23] they revised their earlier value downwards to 1358 W m^{-2}. The measurements made from mountaintops by C. G. Abbot and his co-workers at the Smithsonian Institution are by far the most detailed and extensive for the solar constant and the solar spectrum. They cover a period of nearly half a century. The Smithsonian value, 1352 W m^{-2}[24], is very close to the NASA and ASTM standard.

The uncertainties in the distribution of the solar energy as a function of wavelength are considerably greater than in the solar constant itself. The four different instruments used by the GSFC experimenters on board CV 990 for the same wavelength range did not yield identical curves; there was a certain amount of scatter between them, though the variations were within the estimated error limits of the instruments. There were greater differences between the GSFC curve (weighted average of the four instruments) and the Eppley-JPL filter data[25].

The differences between the NASA/ASTM standard (based on GSFC and Eppley-JPL data) and the solar spectral curves obtained from earlier ground based measurements are considerably greater. Three of these curves and the standard are shown in Figure 6. The most significant variations are in the

spectral range near 0.55μm. This mode of comparison fails to show the spectral differences as distinct from those in the solar constant; and in the wavelength range of low irradiance the curves seem to be identical, though they are far from being so.
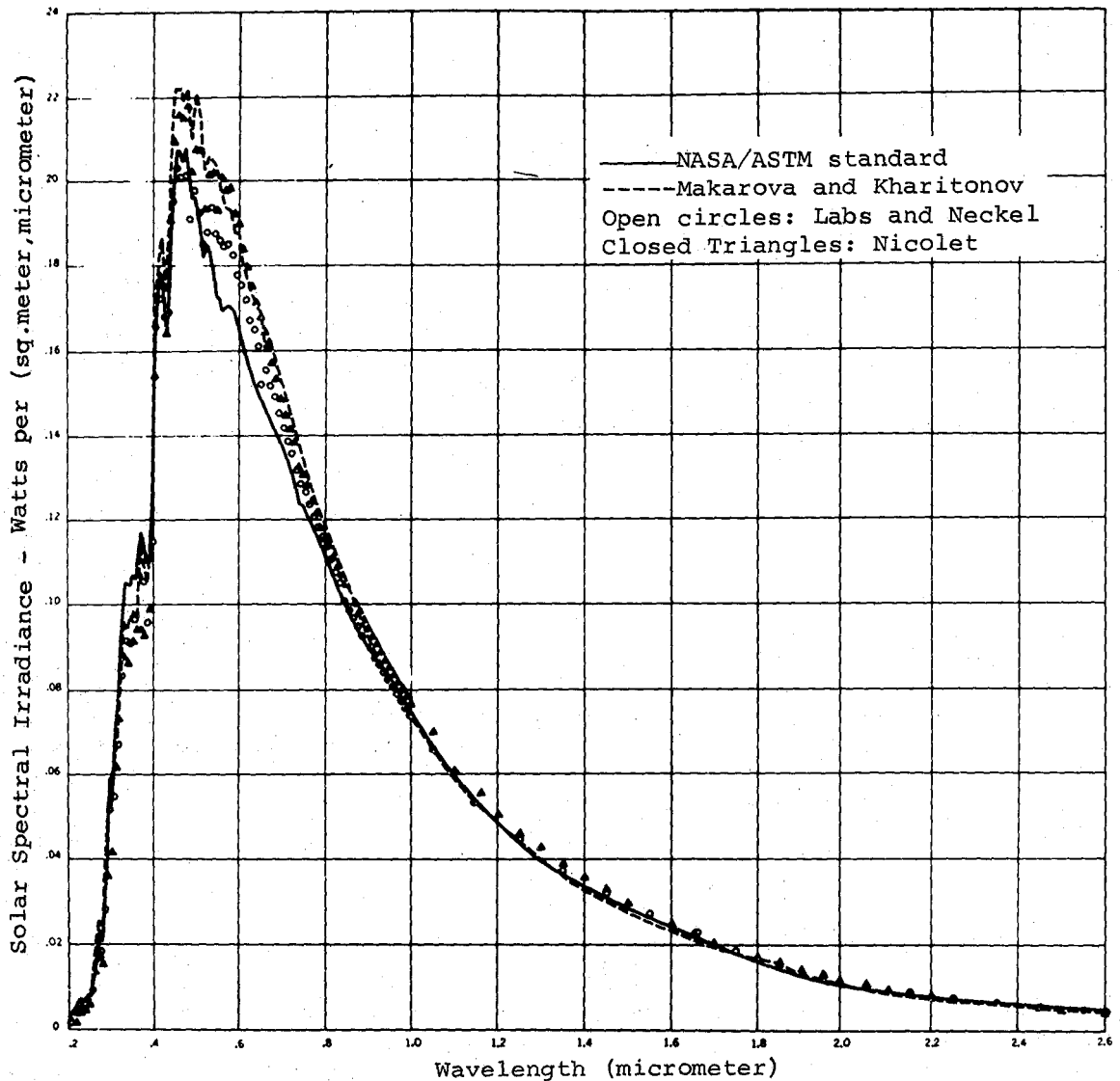
Figure 6. The NASA/ASTM standard curve compared with the curves derived by Makarova and Kharitonov, Labs and Neckel, and Nicolet.

A clearer and more meaningful comparison of the standard curve with that of Labs and Neckel is shown in Figure 7. The Y-axis is the ratio $R = k \cdot P_\lambda'/P_\lambda$, where P_λ is the irradiance as given in the standard table (Table 3) and P_λ' is the irradiance at the same wavelength from Labs and Neckel. k is a normalizing constant which makes the area under the Labs and Neckel curve equal to the standard solar constant, $1353 \, W \, m^{-2}$. The excursions of the ratio curve above and below the 1.0 line show to what extent the Labs and Neckel distribution differs from that of the standard curve.

Similar comparisons with three other spectral curves, those published by F. S. Johnson, Nicolet and Stair and Ellis[26] are shown in Figures 8, 9 and 10 respectively. A comparison of Figures 7, 8 and 9 shows that in the range
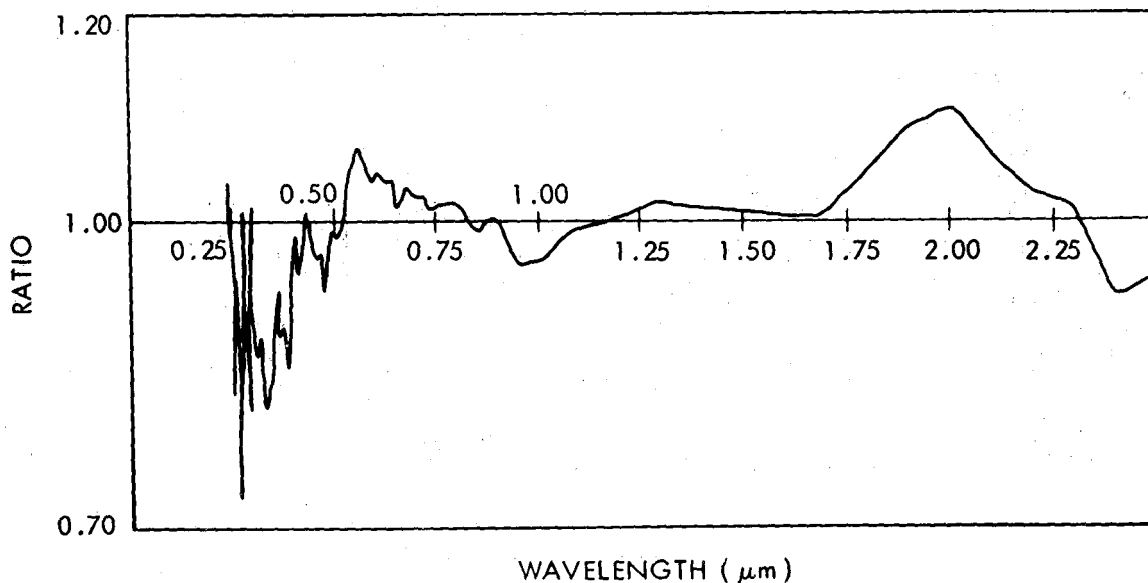
Figure 7. Comparison of NASA/ASTM spectrum with Labs and Neckel spectrum. (Curve gives the ratio of normalized Labs and Neckel values to those of Table III.)

16
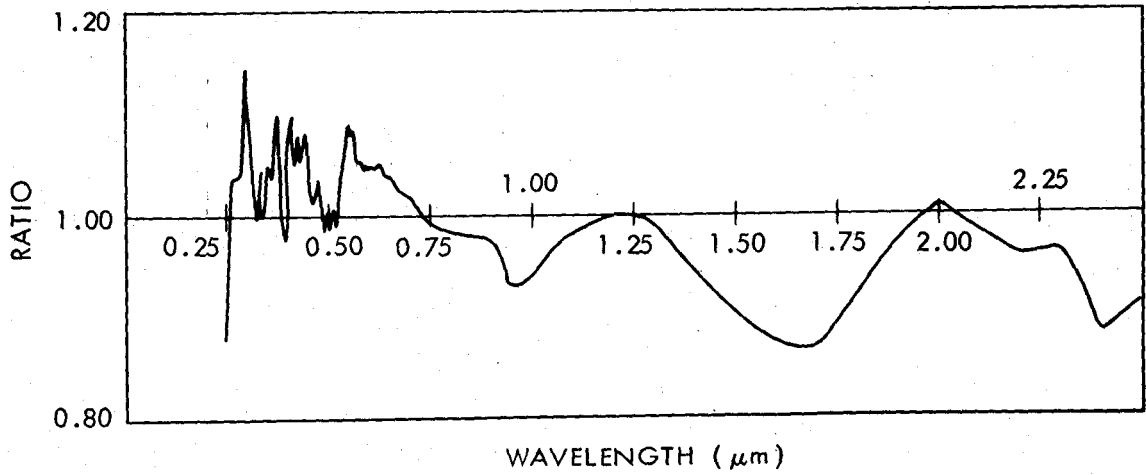
Figure 8. Comparison of NASA/ASTM spectrum to Johnson spectrum. (Curve gives ratio of normalized Johnson values to those of Table III.)
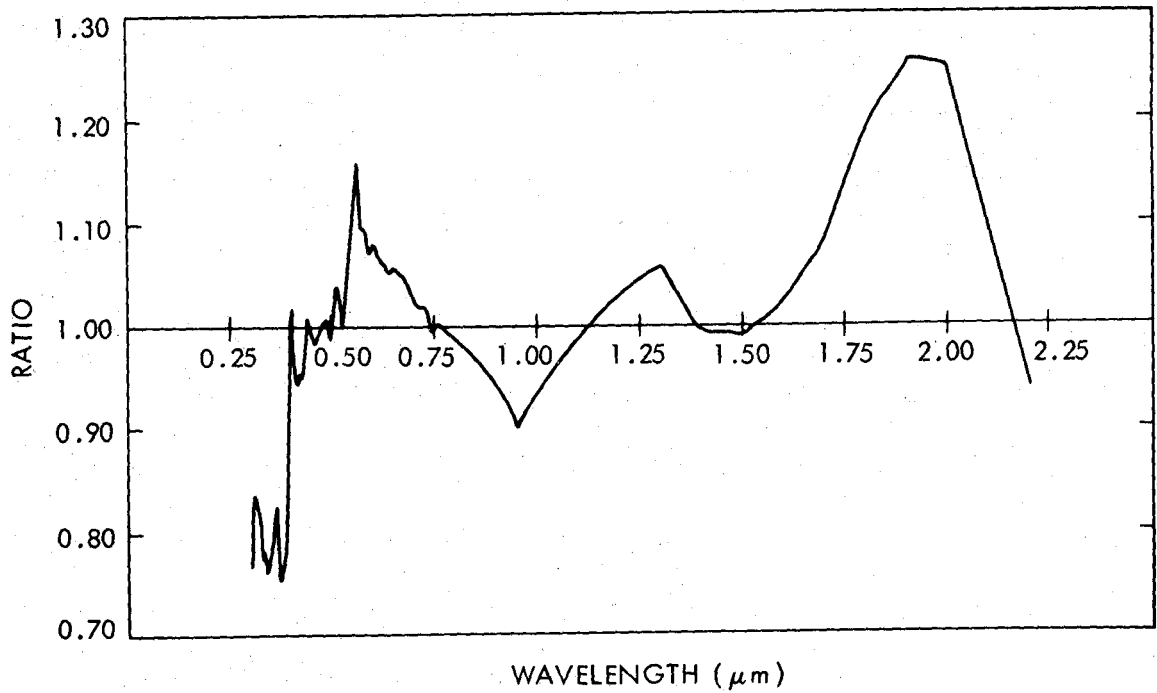
Figure 9. Comparison of NASA/ASTM spectrum to Nicolet spectrum. (Curve gives the ratio of normalized Nicolet values to those of Table III.)
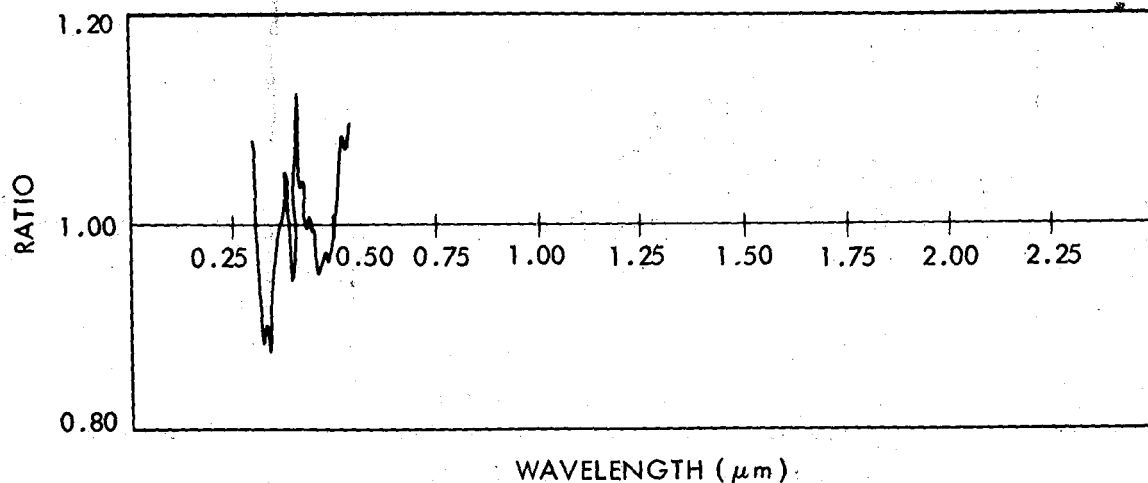
Figure 10. Comparison of NASA/ASTM spectrum to Stair and Ellis spectrum. (Curve gives the ratio of normalized Stair and Ellis values to those of Table III.)

0.25 to 0.45 μm, the Johnson values are higher and those of Labs and Neckel and Nicolet are lower than the standard. It will be recalled that Johnson had scaled Dunkelman and Scolnik's values[27] upward by 8.8%. The values of Labs and Neckel and of Nicolet are low probably because of the difficulty of estimating the solar continuum in a wavelength range which is so rich in Fraunhofer lines. Both Nicolet and Labs and Neckel show a sharp change in the ratio near the Balmer discontinuity, which is not seen in Figures 8 and 10 where the data are based on irradiance of the whole disc rather than on radiance at the center of the disc. The Stair and Ellis curve is of special significance. Two instruments were used, a Leiss monochromator and a filter radiometer. The wavelength range was limited by the photo-multiplier detector to 0.3 to 0.53 μm. The excursions of the ratio line above and below the ratio line are more or less evenly balanced.

18

A wavelength range which has given rise to a certain amount of controversy is from 0.5 to 0.7 μm. In this range the values of Labs and Neckel, Johnson and Nicolet are all higher than the standard values, as shown by Figures 7, 8 and 9. But this is a spectral range where the different instruments of the GSFC CV 990 experiment were in rather close agreement. Confirmation of the standard values was obtained recently from independent sources. Michael Kuhn[28] made measurements at Plateau Station in the Antarctic with differential broad band filters and a pyrheliometer and extrapolated the values to zero air mass. The zero air mass solar irradiance values were respectively 178.9 W m^{-2} and 116.5 W m^{-2} for the wavelength ranges 0.525 to 0.63 μm and 0.63 to 0.71 μm. The corresponding values of the standard table are 178.7 W m^{-2} and 116.5 W m^{-2}, as may be seen by taking the differences of the column $E_{o-\lambda}$ of Table III. Since Table III claims an accuracy of ±5%, this agreement should be considered rather fortuitous. R. Hulstrom (Martin Marietta, Boulder, Colorado)[29] made during 1973 a series of measurements over the range 0.4 to 1.35 μm. His values extrapolated to zero air mass show close agreement with the standard curve over the whole range. The agreement over the range 0.5 to 0.7 μm is particularly striking. Another valuable confirmation is from A. Ångström[30]. His detailed analysis of atmospheric turbidity (β coefficient) covers a period of many years and ground based data of several observers including those of himself and A. Drummond from Mauna Loa. He concludes that the extraterrestrial solar spectrum in the range 0.3 to 0.7 as given in Table III is essentially correct.

19

3. POSSIBLE VARIATIONS IN SOLAR IRRADIANCE AND THEIR EFFECTS

Next question is the variability of the solar energy output. Does the energy output, total and spectral, change with all the other features of the Sun which are known to change? Among the cyclic changes of the Sun the best known is the 11 year sunspot cycle. Figure 11 shows the annual average sunspot numbers from 1760 to 1960. In addition to the 11 year cycle there is the 22 year cycle of solar magnetic field and probably a 90 year cycle of sunspots. There are several intriguing meteorological phenomena which seem to follow the changes in the Sun. J. M. Mitchell[31] presented a very detailed study of this topic at an
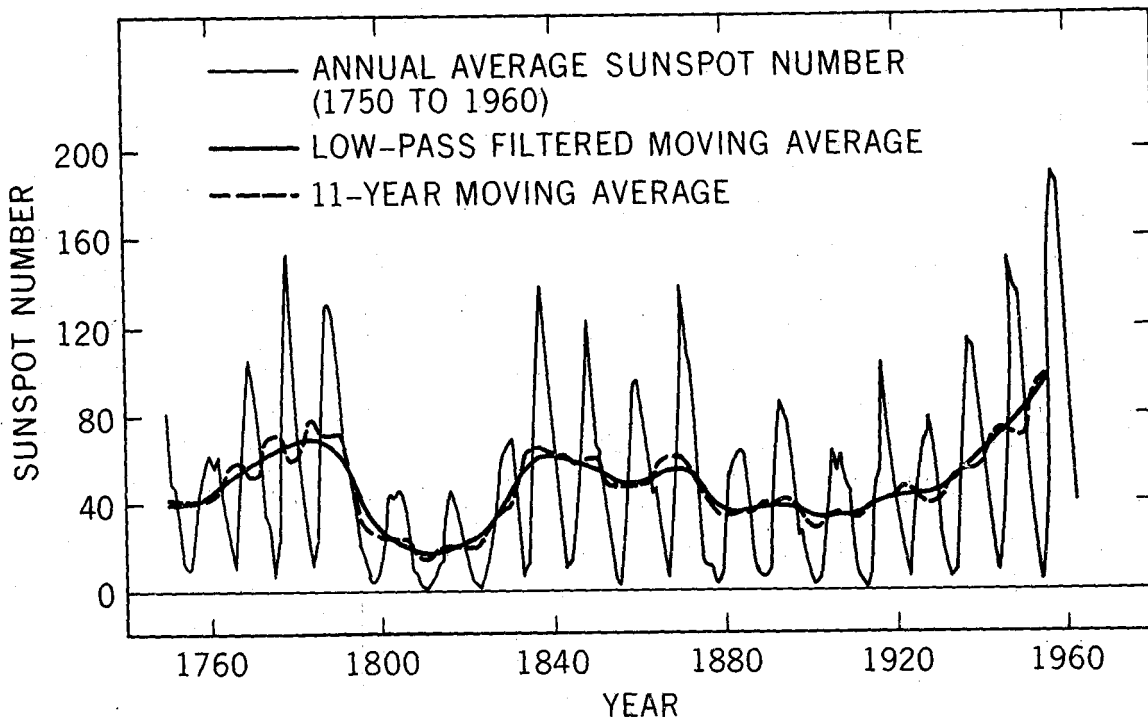
Figure 11. Annual average sunspot number (Zurich number or Wolf number of sunspots) over the period 1750 to 1960.

NCAR symposium in 1965. Among these variations are Etesian winds, wintriness index of the northern hemisphere sea level pattern, the annual march of temperature in different cities of Europe, changes in meridional sea level pressure, growth rings of trees, ozone density, geomagnetism, glacier movement. Add to these, the recurrence of drought in North America every 22 years (solar magnetic cycle) as was pointed out by C. G. Abbot in 1938 and the 11 year pattern in the movement of high pressure systems in Australia as pointed out by E. G. Bowen[32].

Let us look at some of these in more detail. Figure 12 shows the number of days per year when Etesian winds blow over Athens. The annual frequency of Etesian winds from 1893 to 1961 follows the same trends of maxima and minima as the sunspot numbers. That the Earth-atmosphere system reacts to changes in the input energy of the Sun is a well established fact. The density of the ozone layer changes from day to night. The changes in the ionization layers of the upper atmosphere and their dependence on solar phenomena have been studied in great detail because of their direct effects on radio communication. The geomagnetic disturbances have a periodicity of 27 days superposed on an 11-year period, in agreement with the rotational and Wolf number cycles of the Sun[33]. The 11-year cycle of magnetic μ figure is clearly shown on Figure 13. In Figure 14 the charts of magnetic character figure C_i over a period of nine solar rotation cycles are shown one below the other. Long period correlation with sunspot cycles has been observed in such weather related phenomena as
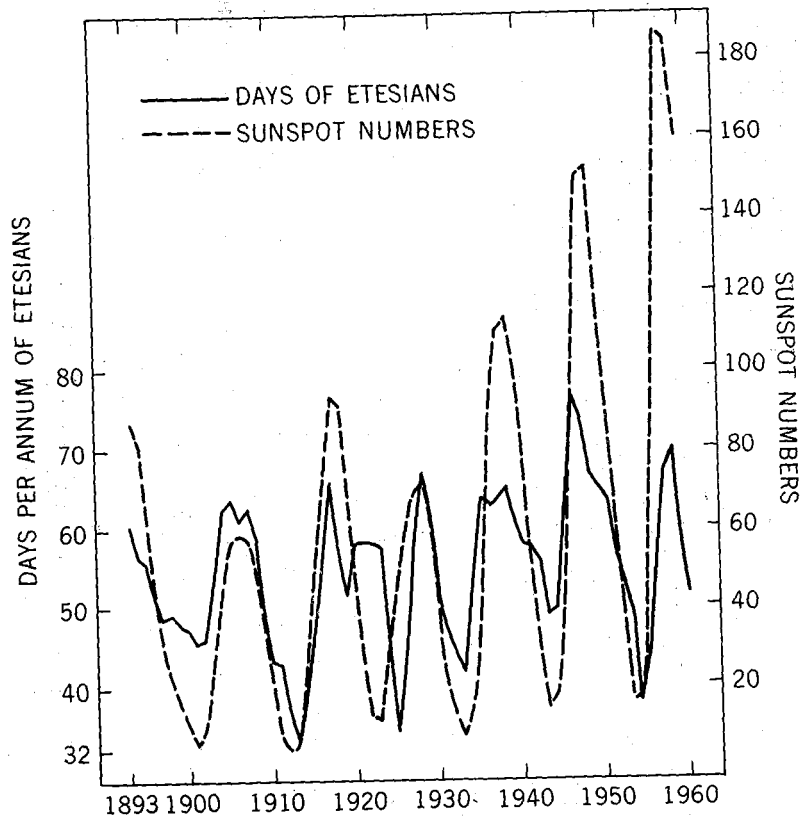
Figure 12. Correlation between annual average of
sunspot numbers and the number of days per
year of Etesian winds.
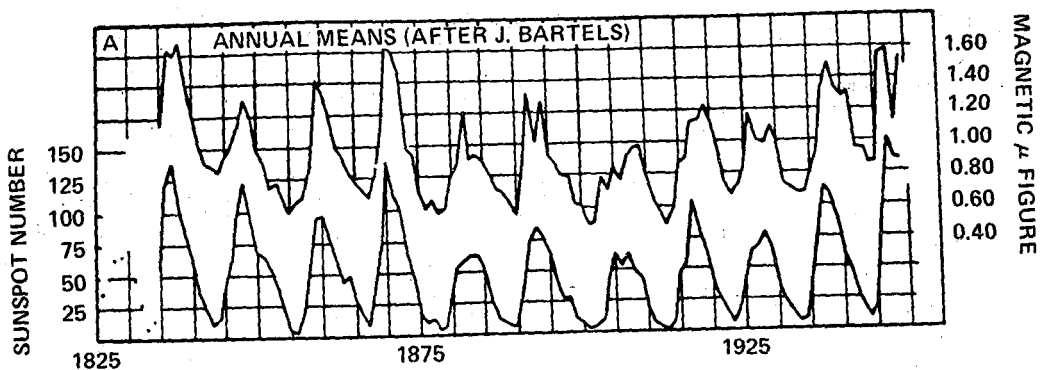
Figure 13. Correlation between geomagnetic disturbance and the 11
year sunspot activity. Upper curve shows the magnetic μ
figure and the lower curve shows the annual mean sunspot number.
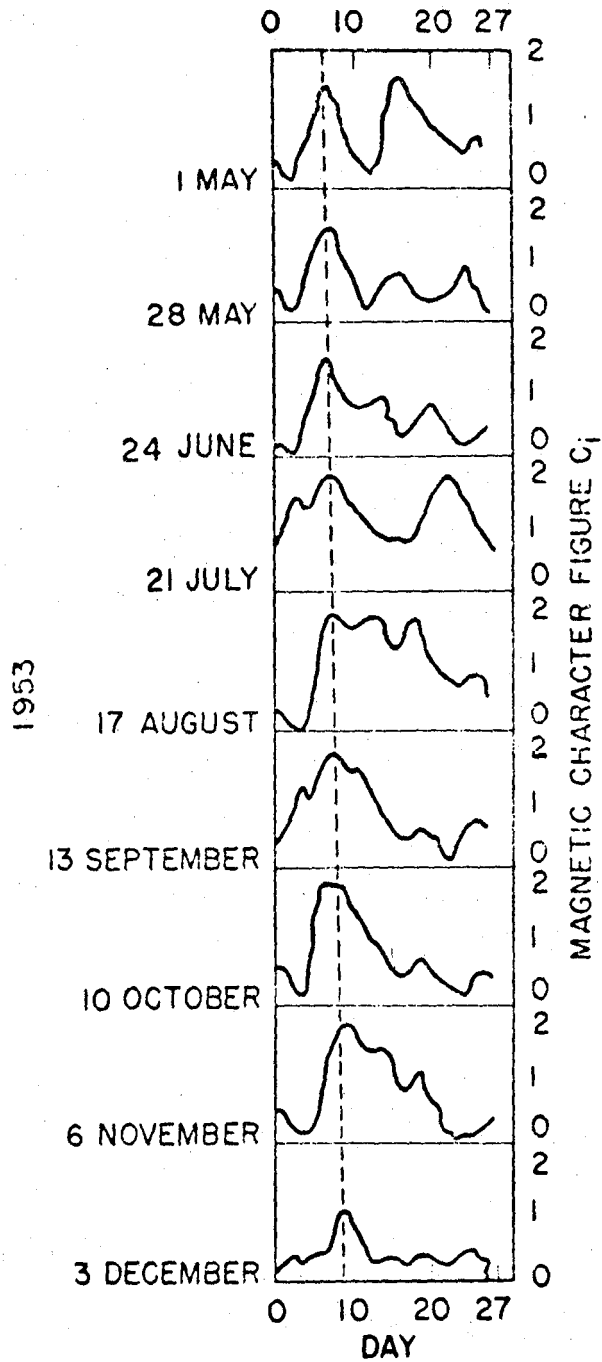
Figure 14. Correlation of geomagnetic disturbance and solar rotation. Curve shows the magnetic character figure C_i as a function of days 1 through 27 over nine solar rotations.

the water level in rivers and lakes, annual growth rings of petrified and living trees, and the advance and retreat of glaciers. Solar events such as flares cause corpuscular emission of which the effects are observed in aurorae, geomagnetic disturbances, changes in cosmic ray flux, increase in ionization of the D layer, possibly localized heating of the atmosphere. Changes in photon flux, though small, apparently act as a trigger mechanism which upsets a delicate energy balance and causes large scale meteorological changes.

Several attempts have been made to determine the variations in solar constant. The most extensive data are those of the Smithsonian Institution. Kondratyev and his co-workers[4] conclude from their balloon data over a six-year period that the maximum value of the solar constant occurs for sunspot numbers between 80 and 100 and that the solar constant decreases by 2 to 2.5 percent during sunspot maximum and minimum. The Lowell Observatory program on the Sun as a variable star[34] shows a gradual increase of the solar constant by 1.4 percent as the sunspot number increases from 2 to 200. Bossolasco and his group[35] analyzed data from four widely separated stations and concluded that the maximum value of the solar constant occurs for Wolf number N about 160, and that the solar constant is significantly lower for $N < 160$ and $N > 160$; the minimum at $270 < N < 330$ is about 15 percent lower. But this conclusion has been disputed by Kondratyev who ascribes the low value to increased atmospheric turbidity caused by nuclear tests. C. G. Abbot and his co-workers of the Smithsonian Institution[36] present a large mass of

24

evidence for variations in the solar constant, for example, a drop of 4 percent when a large sunspot crosses the disc, a similar decrease accompanied by magnetic storms and West Indian hurricanes, periodicities related to 273 months (period of the solar magnetic cycle) and related weather phenomena.

While there is a great deal of literature about changes in the solar constant and their effects on weather, there is hardly any mention of changes in spectral distribution in the visible and near IR where the energy output is the greatest. The reason is not that changes do not exist, but they are totally unknown and unexplored. Almost all solar energy effects on the atmosphere and the Earth are wavelength dependent. Localized radiation balance and transport of large masses of air, increase of pollution and changes in sink mechanisms, the making of weather and climate and the modelling required for prediction of weather, changes in ozone and their erythemal effects on humans, all depend on some limited portions of the solar spectrum more than on others. The atmosphere is far from being a neutral density filter, nor is the land and ocean surface of the Earth an achromatic absorber. The Earth albedo spectrum is different from the solar spectrum. Ozone production is due to solar UV. Photosynthesis essential for all life support is due to wavelength bands centered round 0.44 and 0.75 μm. Other resonance phenomena are photomorphogenic responses like seed and flower development, shape and size of leaves, plant height, leaf movements as in mimosa; the associated wavelengths are 0.66 and 0.73 μm. Absorption by water vapor with all its major effects on the making of weather is

25

in narrow wavelength bands, all beyond 0.7 μm, as shown on Figure 3. This is the more poorly known part of the solar spectrum.

4. A MEASUREMENT PROGRAM FOR SOLAR ENERGY IN SPACE

An obvious conclusion from these discussions of the state of our knowledge on the solar constant and solar spectrum and the relative lack of knowledge about the variations of these parameters is that a strong effort should be made for the measurement of solar irradiance, both total and spectral, with considerably greater accuracy and precision and that such measurements should be made on a continuing basis. During the first decade of the space age it has been possible to measure solar irradiance from above all or almost all of the atmosphere. Except for the Mars Mariner, the observing platforms were spacecraft and balloons. Satellites were not used for this purpose since the degree of accuracy aimed at is such that the experimental package should be retrieved after the flight for recalibration and for checking possible degradation of the optical components and detectors.

A project is now being developed for more precise and accurate determination of solar irradiance on a continuing basis. The objective is to monitor the solar constant with an accuracy of better than one percent and the solar spectral irradiance with an accuracy better than three percent. The variations of these parameters will be determined with a precision considerably greater than the absolute accuracy. The instrument package will be mounted in a U-2 aircraft which has a cruising altitude of 20 km. Observing time per flight will be about

six hours. The instrument package will consist of a medium resolution prism monochromator for the spectrum and a thermopile detector for the total energy.

A schematic of the instrument package is given in Figure 15. Sun's light enters an integrating sphere A through an aperture on its top B. The total irradiance is measured by a thermopile detector C and the spectral irradiance by a monochromator D. The mirror E focusses the light to the entrance slit F. It is chopped by a tuning fork chopper G, collimated by the mirror H, and spectrally dispersed by the prism I. The Littrow mirror J returns the light to the prism for doubling the dispersion. The concave mirror H focusses the light to the exit slit K, from which it falls on another focussing mirror L. The beam splitter M transmits the light to the two detectors, a photodiode N for the wavelength range 0.25 to 1.1 μm and a lead sulfide tube or a thermopile for the wavelength range $\lambda > 0.7 \mu$m.

The instrument package will be provided with a tracking mechanism so that it will view constantly the Sun and a small portion of the circumsolar sky. It will be mounted in the Q-bay of the U-2 aircraft where a pressure of 350 millibars and a temperature range of 5°C to 25°C will be maintained. The residual atmosphere above the aircraft at 20 km is about 5% of what it is at sea level and the water vapor above the aircraft is 0.05% of the average amount of precipitable water in the atmosphere. About 50% or more of the ozone is above the aircraft so that the lower limit of the observable spectrum is 0.27 μm. The upper limit is 2.6 μm with quartz optics and 4.0 μm with sapphire optics. Since
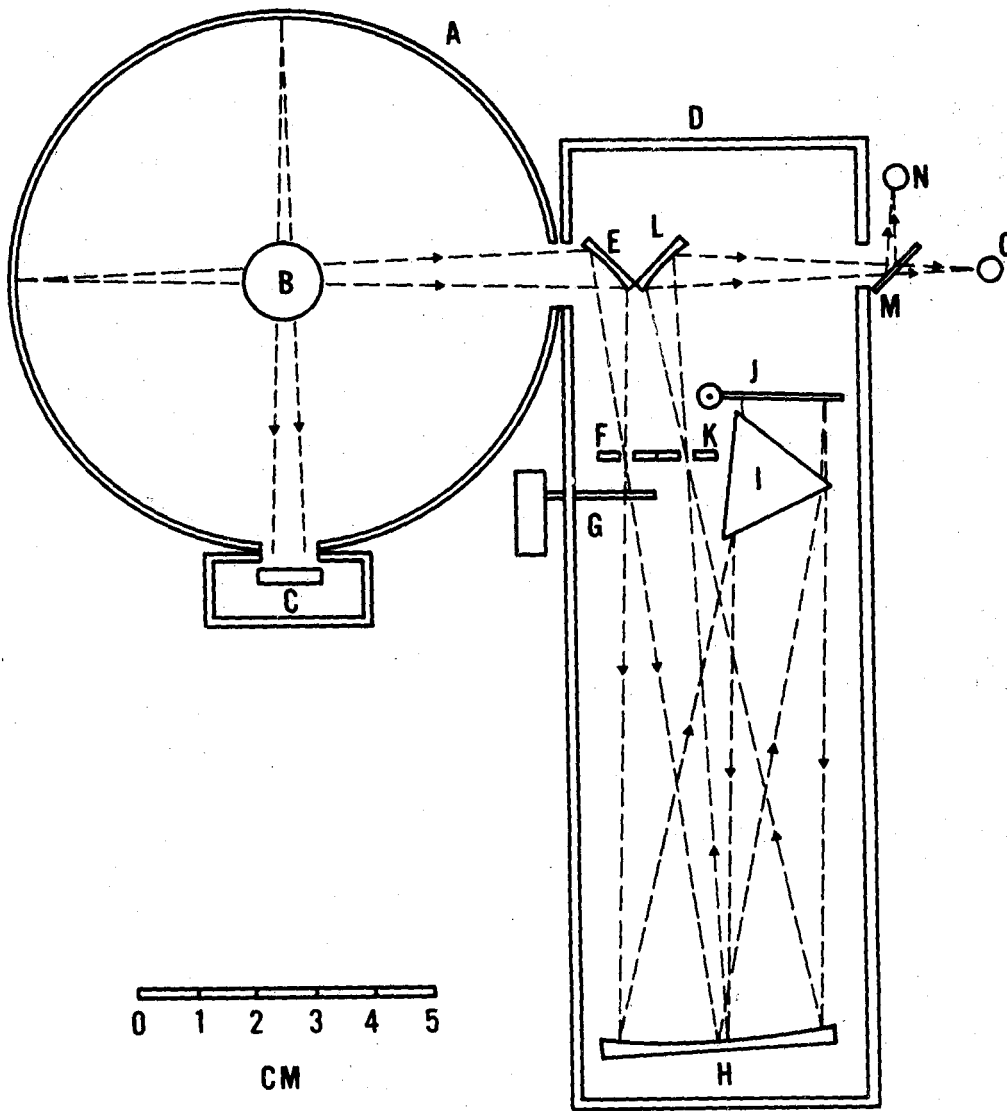
Figure 15. Optical schematic of Solar Energy Monitor in
Space (SEMIS). Sunlight is received by an integrating sphere.
Total energy is measured by a detector C and the
spectrum is scanned by a prism monochromator D.

there is a certain amount of residual atmosphere above the aircraft, extrapolation to zero air mass will be made by measuring the solar energy at zenith angles varying between 15° and 60°. The instrument will be sufficiently light weight and compact so that it can be flown "piggy-back" on all routine missions of the U-2 aircraft.

The U-2 measurements will permit the development of a more reliable and rugged instrument for deployment on the Space Shuttle which will be in operation in the 80's. A floating laboratory above the ozonosphere and all other atmospheric absorbents, with manned instruments and on-board calibration, with few constraints as to weight, size and power, with long observation periods, total and spectral irradiance of the Sun can be determined with sufficient accuracy and resolution. This will provide an answer to many questions about the Sun's energy output which have often been raised but never adequately answered.

5. ACKNOWLEDGMENTS

REFERENCES

1. D. G. Murcray: Balloon Borne Measurements of the Solar Constant. University of Denver Report AFCRL-69-0070 (Denver, Colorado), Jan. 1969

   D. G. Murcray, et al.: The Measurement of the Solar Constant from High Altitude Balloons, University of Colorado, Report AFCRL-68-0452 (Denver, Colorado), Aug. 1968.

2. M. P. Thekaekara, R. Kruger, and C. H. Duncan: Solar Irradiance Measurements from a Research Aircraft. Appl. Opt. 8 (8), 1713-1732 (1969).

   M. P. Thekaekara, ed.: The Solar Constant and the Solar Spectrum Measured from a Research Aircraft. NASA TR R-351, Washington, D.C. (1970).

3. J. A. Plamondon: The Mariner Mars 1969 Temperature Control Flux Monitor. Jet Propulsion Laboratory Space Programs Summary 37-59, vol. 3, pp. 162-168, Oct. 1969.

4. K. Ya. Kondratyev, and G. A. Nikolsky: Solar Radiation and Solar Activity. Quarterly J. Royal Meteorological Society, vol. 96, no. 3, pp. 509-522, July 1970.

   K. Ya. Kondratyev, et al.: Direct Solar Radiation up to 30 km and Stratification of Attenuation Components in the Stratosphere. Applied Optics, vol. 6, no. 2, pp. 197-207, Feb. 1967.

5. A. J. Drummond, et al.: New Value of the Solar Constant of Radiation. Nature, vol. 218, no. 5138, pp. 259-261, April 20, 1968.

6. A. J. Drummond, and J. R. Hickey: The Eppley-JPL Solar Constant Measurement Program. Solar Energy, vol. 12, no. 2, pp. 217-232, Dec. 1968.

   E. G. Laue, and A. J. Drummond: Solar Constant: First Direct Measurements. Science, vol. 161, no. 3844, pp. 888-891, Aug. 1968.

7. A. J. Drummond, et al.: The Calibration of Multichannel Radiometers for Application in Spacecraft and Space Simulation Programs. Proceedings International Astronautical Federation 18th Congress, Belgrade, vol. 2, pp. 407-422, 1967. (Pergamon Press, New York, 1968.)

8. R. C. Willson: Active Cavity Radiometric Scale, International Pyrheliometric Scale and Solar Constant, J. Geophys. Research, vol. 76, no. 19, pp. 4325-4340, 1971.

9. D. F. Heath: Observations on the Intensity and Variability of the Near Ultraviolet Solar Flux from the Nimbus III Satellite. J. Atmospheric Sciences, vol. 26, no. 5, pt. 2, pp. 1157-1160, Sept. 1969.

10. H. E. Hinteregger: The Extreme Ultraviolet Solar Spectrum and Its Variation During a Solar Cycle. Ann. Geophysique, vol. 26, no. 2, pp. 547-554, 1970.

11. F. J. Shimabukoro, and J. M. Stacey: Brightness Temperature of the Quiet Sun at Centimeter and Millimeter Wavelengths. Astrophys. J., vol. 152, no. 6, pp. 777-782, June 1968.

12. Anon.: Solar Electromagnetic Radiation, NASA Space Vehicles Design Criteria, NASA, SP 8005, NASA, Washington, D.C., May 1971.

13. Anon.: Standard Specification for Solar Constant and Air Mass Zero Solar Spectral Irradiance, ASTM Standard E 490-73a, 1974 Annual Book of ASTM Standards, Part 41, ASTM, Philadelphia, 1974.

14. F. S. Johnson: The Solar Constant. J. Meteorology, vol. 11, no. 6, pp. 431-439. Dec. 1964.

15. J. Kasper, in American Institute of Physics Handbook, 3rd Edn. McGraw Hill Book Co., Inc., New York, p. 6-216, 1972.

16. L. Elterman: UV, Visible and IR Attenuation for Altitudes to 50 km, 1968 AFCRL-68-0153, Office of Aerospace Research, U.S. Air Force, 1968.

17. D. M. Gates, and W. J. Harrop: Infrared Transmission of the Atmosphere to Solar Radiation, App. Optics, 2, p. 887, 1963.
   D. M. Gates: Near Infrared Atmospheric Transmission to Solar Radiation, J. Opt. Soc. Am., 50, p. 1299, 1960.

18. M. Nicolet: Sur le Probleme de la Constante Solaire. Ann. d'Astrophysique, vol. 14, no. 3, pp. 249-265, July-Sept. 1951.

19. R. Stair, and R. G. Johnston: Preliminary Spectroradiometric Measurements of the Solar Constant. J. Res. Nat. Bur. Stand., vol. 57, no. 4, pp. 205-211, Oct. 1956.

20. E. A. Makarova: A Photometric Investigation of the Energy Distribution in the Continuous Solar Spectrum in Absolute Units. Soviet Astronomy—AJ, vol. 1, no. 4, pp. 531-546, April 1957.

21. E. A. Makarova, and A. B. Kharitonov: The Energy Distribution in the Solar Spectrum and the Solar Constant (in Russian), Nauka Publishing House, Moscow, 1972.

22. D. Labs, and H. Neckel: The Radiation of the Solar Photosphere from 2000 A to 100 μ. Zeitschrift fur Astrophysik, vol. 69, pp. 1-73, 1968.

23. D. Labs, and H. Neckel: Transformation of the Absolute Solar Radiation Data into the International Practical Temperature Scale of 1968, Solar Physics, 15, pp. 79-87, 1970.

24. L. B. Aldrich, and W. H. Hoover: The Solar Constant. Science, vol. 116, no. 3024, p. 3, Dec. 1952.

25. M. P. Thekaekara, and A. J. Drummond: Standard Values for the Solar Constant and its Spectral Components. Nature, Physical Sciences, vol. 229, no. 1, pp. 6-9, Jan. 4, 1971.

26. R. Stair, and H. T. Ellis: The Solar Constant Based on New Spectral Irradiance Data from 3100 to 5300 Ångströms. J. of Appl. Meteorology, vol. 7, no. 8, p. 635, Aug. 1968.

27. L. Dunkelman, and R. Scolnik: Solar Spectral Irradiance and Vertical Attenuation in the Visible and Ultraviolet. Opt. Soc. Amer. J., vol. 49, no. 4, pp. 356-367, April 1959.

28. Private communication, J. Hickey, Sept. 11, 1972; M. Kuhn, Nov. 15, 1973.

29. R. L. Hulstrom: Instrumentation, Measurements and Analysis of Solar Energy, paper presented at the NOAA/NSF Workshop, Silver Spring, Md., Nov. 29, 30, 1973.

30. Private Communication, A. Ångström, Jan. 17, 1973.

31. J. M. Mitchell: The Solar Inconstant, National Center of Atmospheric Research, Tech. Note TN-8, 156, 1965.

32. E. G. Bowen, Kidson's Relationship between Sunspot Number and the Movement of High Pressure Systems in Australia, presented at the GSFC Symposium on Solar Activity, November 7, 8, 1973.

33. C. F. Campen, et al.: Ed., Handbook of Geophysics (AFCRL) MacMillan Co., New York, pp. 10-5 and 17-11, 1960.

34. H. L. Johnson, and B. Iriarte: The Sun as a Variable Star, Lowell Observatory, Bulletin No. 96, vol. 4, no. 8, pp. 99-104, 1959.

35. M. Bossalasco, et al.: Solar Constant and Sunspots, Pure and Ap. Geophysics, (Pageoph), vol. 62 (1965/III), pp. 207-214, 1965.

36. C. G. Abbot, et al.: Annals Astrop. Obs. Smith. Inst. 6, 1942.

L. B. Aldrich: The Solar Constant and Sunspot Numbers, Smith., Misc. Coll. 104 (12) pp. 1-5, 1945.

L. B. Aldrich, and W. H. Hoover, Ann. Astroph. Obs., Smiths. Inst. 7, 1954.

FIGURE CAPTIONS

Fig. 1.   The NASA/ASTM standard curve of extraterrestrial solar spectral

irradiance, 0.2 to 2.6 μm.

Fig. 2.   The extraterrestrial solar spectrum from X-rays to radio waves.

Fig. 3.   Solar irradiance spectra at ground level for air mass 1, 4, 7 and 10,

compared to the standard curve - computed values.

Fig. 4.   Solar spectrum obtained with a Perkin-Elmer monochromator, air

mass zero, 3000 - 4000 A.

Fig. 5.   Solar spectrum obtained with a Perkin-Elmer monochromator, air

mass zero, 3600 - 6100 A.

Fig. 6.   The NASA/ASTM standard curve compared with the curves derived

by Makarova and Kharitonov, Labs and Neckel, and Nicolet.

Fig. 7.   Comparison of NASA/ASTM spectrum with Labs and Neckel spectrum.

(Curve gives the ratio of normalized Labs and Neckel values to those

of Table III.)

Fig. 8.   Comparison of NASA/ASTM spectrum to Johnson spectrum.   (Curve

gives ratio of normalized Johnson values to those of Table III.)

Fig. 9.   Comparison of NASA/ASTM spectrum to Nicolet spectrum.   (Curve

gives the ratio of normalized Nicolet values to those of Table III.)

Fig. 10. Comparison of NASA/ASTM spectrum to Stair and Ellis spectrum.

(Curve gives the ratio of normalized Stair and Ellis values to those of

Table III.)

Fig. 11. Annual average sunspot number (Zurich number or Wolf number of sunspots) over the period 1750 to 1960.

Fig. 12. Correlation between annual average of sunspot numbers and the number of days per year of Etesian winds.

Fig. 13. Correlation between geomagnetic disturbance and the 11 year sunspot activity. Upper curve shows the magnetic μ figure and the lower curve shows the annual mean sunspot number.

Fig. 14. Correlation of geomagnetic disturbance and solar rotation. Curve shows the magnetic character figure C_i as a function of days i through 27 over nine solar rotations.

Fig. 15. Optical schematic of Solar Energy Monitor in Space (SEMIS). Sunlight is received by an integrating sphere. Total energy is measured by a detector C and the spectrum is scanned by a prism monochromator D.